Interaction energies of perturbed-angular-correlation probes with impurities in Ag and Pd

T. Hoshino
Department of General Education, College of Engineering, Shizuoka University, Hamamatsu 432, Japan

B. Drittler, R. Zeller, and P. H. Dederichs
Institut für Festkörperforschung, Forschungszentrum Jülich, D-5170 Jülich, Germany
(Received 19 November 1991)

We present systematic *ab initio* calculations of the nearest-neighbor interaction energies of perturbed-angular-correlation (PAC) probe atoms (^{99}Rh, ^{100}Pd, ^{111}In) with 4*d* and 5*sp* impurity atoms (Zr–Sb, with $Z=40-51$) in Ag and Pd crystals. The calculations are based on local-density theory and apply the Korringa-Kohn-Rostoker Green's-function method for spherical potentials. The full nonspherical charge density is evaluated to calculate the double-counting contributions to the total energy. The present calculations reproduce very well most of the available experimental interaction energies of probe-impurity pairs in the two metal hosts. It is shown that the interactions of the 4*d*-4*d* probe-impurity pairs in Ag and Pd can be understood by considering both the changes of the *d* bond and the repulsive energies between the different atomic rearrangement of isolated probe and impurity atoms and of the probe-impurity pair. On the other hand, the interactions of the 5*sp*-5*sp* probe-impurity pairs as well as 4*d*-5*sp* and 5*sp*-4*d* in Ag can be explained by a change in the electrostatic interaction induced by the changes of the nuclear charges of the probe and impurity atoms with respect to the host atom. It is found that the calculated interaction energies of the *Ag* ^{100}Pd*X* and *Pd* ^{99}Rh*X* ($X=$Zr–Sb) systems, where the probe atoms are neighboring elements of the host atoms, can very well be reproduced by the Miedema-Królas model. Some comments are also made on the experimentally obtained attraction for the *Pd* ^{99}Rh*X* ($X=$Cd–Sb) systems, which cannot be reproduced by the present calculations.

I. INTRODUCTION

The interaction of impurity pairs in dilute alloys has been the subject of numerous experimental studies in the last decade. The knowledge of the impurity-impurity interaction is indispensable to the understanding of many basic physical processes, such as diffusion, short-range order, segregation, ordering, etc. It has recently been demonstrated that hyperfine interaction methods such as the Mössbauer effect and perturbed angular correlation (PAC), are powerful tools to study the impurity interactions.[1] In particular, PAC spectroscopy has the ability to deal with very low probe-atom concentrations ($\sim 10^{-8}$) without restriction the temperature. The interaction energies of the probe-impurity pairs are determined from the temperature-dependent measurement of the probe-impurity pair concentrations. Up to now, four PAC probes (^{99}Rh, ^{100}Pd, ^{111}Ag, and ^{111}In) have been used to investigate the impurity-impurity interactions in seven metals (Fe, Ni, Cu, Rh, Pd, Ag, and Au) and experimental data for about 50 impurity pairs in these hosts are summarized in the review of Królas.[1]

From the theoretical point of view, the calculation of impurity-impurity interaction energies is an especially difficult problem since one must treat a very small change of the total energies arising in the atomic rearrangement from the initial state of two isolated impurities to the final state of the impurity pair. Blandin, Deplante, and Friedel performed jellium-type calculations to discuss qualitatively the chemical trend of the *sp-sp* impurity interactions in nontransition metals and showed the importance of the electron charge redistribution induced by the change of the nuclear charge of both the impurities with respect to the host atom.[2] Based on the same model, Deplante and Blandin also calculated the interactions between vacancies and 3*d* and 4*sp* impurities in Cu.[3] On the other hand, in order to predict the impurity-impurity interaction energies in a large variety of dilute alloys, including alloys based on the transition-metal elements, Królas[4] developed a phenomenological model using the solution energies obtained by the semiempirical model of Miedema *et al.*[5,6] Only recently were realistic *ab initio* calculations carried out by Klemradt *et al.* to study the vacancy-impurity interactions in Cu, Ni, Ag, and Pd.[7,8] These calculations are based on local-density-functional theory[9] and apply the Korringa-Kohn-Rostoker (KKR) Green's-function method for impurities together with a recently developed accurate total-energy formalism.[10] The interaction energies of a vacancy with the impurities, obtained from experiments such as positron-annihilation and diffusion-coefficient measurements, have been very well reproduced by the calculations.

In this paper, we use the same method to study the interaction energies of the PAC probes (^{99}Rh, ^{100}Pd, and ^{11}In) with 4*d* and 5*sp* impurities (Zr–Sb) in Ag and Pd. We have chosen this combination of hosts, probe atoms and impurities, which all belong to the same row in the Periodic Table, in order to minimize the lattice-misfit effects which are out of the scope of the present calculations. We believe that, for the systems considered here,

the additional contribution to interaction energies due to lattice relaxations is not of major importance and can be neglected. Ag is considered as a prototype of free-electron-like hosts and Pd as a prototype of transition metals. Thus, the present paper will give systematic *ab initio* results for the probe-impurity interactions in two different hosts and for a large range of chemically different probe and impurity atoms. We also elucidate the physical mechanism governing the chemical trends of the interactions.

In Sec. II, we describe the characteristic features of the present calculational method. In Sec. III, we discuss the results of the nearest-neighbor interaction energies of the PAC probes (^{99}Rh, ^{100}Pd, and ^{111}In) with the impurities (Zr–Sb) in Ag. We note that the present calculations reproduce the available experimental data very well. It is shown that the calculated results for the 4*d*-4*d* (^{99}Rh-*X* and ^{100}Pd-*X*, X=Zr–Pd) interaction energies in Ag can be understood by a simple model including two contributions, the *d*-bond energy due to the covalent interaction between two 4*d* atoms on the nearest-neighbor sites and the change of the repulsive energy between the ion cores.[11,12] On the other hand, it is shown that the present results for 5*sp*-5*sp* (^{111}In-*X*, X=Cd–Sb), 4*d*-5*sp* (^{99}Rh-*X* and ^{100}Pd-*X*, X=Cd–Sb) and 5*sp*-4*d* (^{111}In-*X*, X=Zr–Pd) impurity pairs can be basically explained by jellium calculations taking into account only the electrostatic interaction induced by the nuclear-charge changes of the impurity and probe atoms. In Sec. IV, we discuss the calculated results for the interaction energies of the PAC probes (^{99}Rh and ^{11}In) with the impurities (Zr–Sb) in Pd. We note that the calculated results agree with the experimental result of ^{111}In-Ag, but completely disagree with those of ^{99}Rh-*X* (X=Cd–Sb) pairs. Some possibilities to account for the discrepancy are also discussed.

In Sec. V, we will examine the efficiency of the Miedema-Królas model[4–6] where the interaction energy between the probe and impurity in the metals is expressed by the three solution energies of the corresponding alloys. We summarize the main results of the present paper in Sec. VI.

II. METHOD OF CALCULATION

We describe the calculational procedure only briefly, as it is the same as the one used by Klemradt *et al.*[8] The calculations are based on the Korringa-Kohn Rostoker Green's-function method for the impurity calculations[9] and on a recently developed accurate total-energy formalism.[10] In the KKR Green's-function method, the Green's function of the system is expanded in each cell into radial eigenfunctions of the local potential, assumed to be spherically symmetric within the Wigner-Seitz spheres. For the spherical potentials we use the $l=0$ component of the full cell potential which is constructed from the full cell charge density. All the multiple-scattering information is contained in the structural Green's-function matrix $G_{LL'}^{nn'}(E)$, which is related to the ones, $\mathring{G}_{LL'}^{nn'}(E)$, of the ideal crystal by a Dyson equation,

$$G_{LL'}^{nn'}(E)=\mathring{G}_{LL'}^{nn'}(E)+\sum_{n'',L''}\mathring{G}_{LL''}^{nn''}(E)\Delta t_{l''}^{n''n'}(E)G_{L''L'}^{n''n'}(E)\ , \qquad (2.1)$$

where $\Delta t_{l''}^{n''}(E)=t_{l''}^{n''}(E)-\mathring{t}_{l''}^{n''}(E)$ is the difference from the host t matrix $\mathring{t}_{l''}^{n''}(E)$. The rank of G is determined by the number of perturbed potentials and the number of angular momenta taken into account.

For the present impurity system, we calculate self-consistently all preturbed potentials in the impurity cluster shown in Fig. 1. It contains 20 atoms with nine inequivalent sites in a fcc lattice; two impurities situated at the nearest-neighbor sites 1 and 2 and 18 host atoms on the sites 3–9 being nearest neighbors to at least one of the impurity atoms. The maximum angular momentum, $l_{\max}$, for the Green's function is chosen to be 3. It was shown in Ref. 10 that both approximations are sufficient to obtain reliable total energies. The change of the integrated density of states, necessary to calculate the change of the single-particle energies induced by the impurities, is determined by Lloyd's formula[10] which analytically sums all perturbations of the wave functions over the whole infinite space. The energy integration is performed by a contour integral in the complex energy plane.[13] The double-counting contributions for both the Coulomb and the exchange energies are calculated by use of the full anisotropic charge density in each Wigner-Seitz cell.[8,14] The integrations over the exact faceted Wigner-Seitz cell can be performed by introducing a Heaviside function, which is equal to one inside and zero outside a cell, expanded by spherical harmonics within the circumscribing sphere of the Wigner-Seitz cell. We apply the density-functional theory in the local-density approximation of von Barth and Hedin with the parameters as given by Moruzzi, Janak, and Williams.[15]

The interaction energy $E_{\rm int}$ between the probe atom *B* and the impurity atom *C* in the hose *A* is defined as the total-energy difference between two states: (1) the final state where the probe atom *B* and the impurity atom *C* are located at nearest-neighbor sites 1 and 2, and (2) the

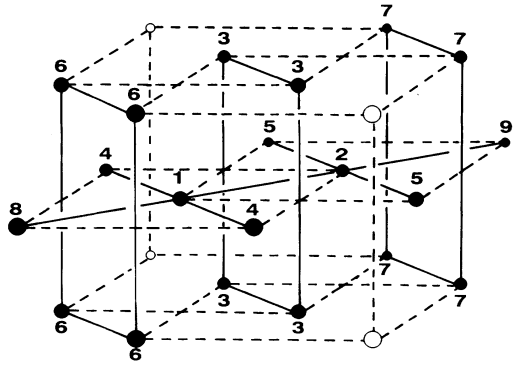

FIG. 1. The 20-atom cluster of C_{2v} symmetry used in the present calculations. All the atoms are on fcc sites. The nine kinds of sites are shown; two impurity sites (1,2) in the center and seven nearest-neighbor sites (3–9) adjacent to the impurity sites.

initial state where both atoms are infinitely far away. For the latter case we have to perform two independent calculations, one with the impurity B on site 1 and a host atom A on site 2 and another one with the impurity C on site 2 and a host atom A on site 1. Thus, $E_{\rm int}$ is given by

$$E_{\rm int}=\Delta E_{BC}-\Delta E_{BA}-\Delta E_{AC}\ , \tag{2.2}$$

$$\Delta E_{BC}=E_{BC}-E_{AA}\ , \tag{2.3a}$$

$$\Delta E_{BA}=E_{BA}-E_{AA}\ , \tag{2.3b}$$

$$\Delta E_{AC}=E_{AC}-E_{AA}\ , \tag{2.3c}$$

where E_{XY} represents the total energy of the system with the X-Y pair in the center of the cluster and ΔE_{XY} is the excess energy with respect to the energy of the ideal A crystal. All energies E_{XY}'s are calculated using the same 20-atom geometry shown in Fig. 1.

III. CALCULATED RESULTS OF THE PROBE-IMPURITY INTERACTION IN Ag

In this section we discuss the calculated results for the nearest-neighbor interaction energies of the PAC probes (^{99}Rh, ^{100}Pd, ^{111}In) with 4d and 5sp impurities (Zr–Sb) in Ag. Figure 2 and Table I show the calculated interaction energies as well as available experimental values.[16–20] Positive energies mean repulsive interaction between the probe and impurity, negative attractive ones. We note that the agreement between the calculated and experimental values is very gratifying. It should also be noted in Fig. 2 that the calculated results for the ^{99}Rh and ^{100}Pd probes are similar to each other, but very different from those of the ^{111}In probe. From the characteristics of the chemical trends found in the calculation, the probe-

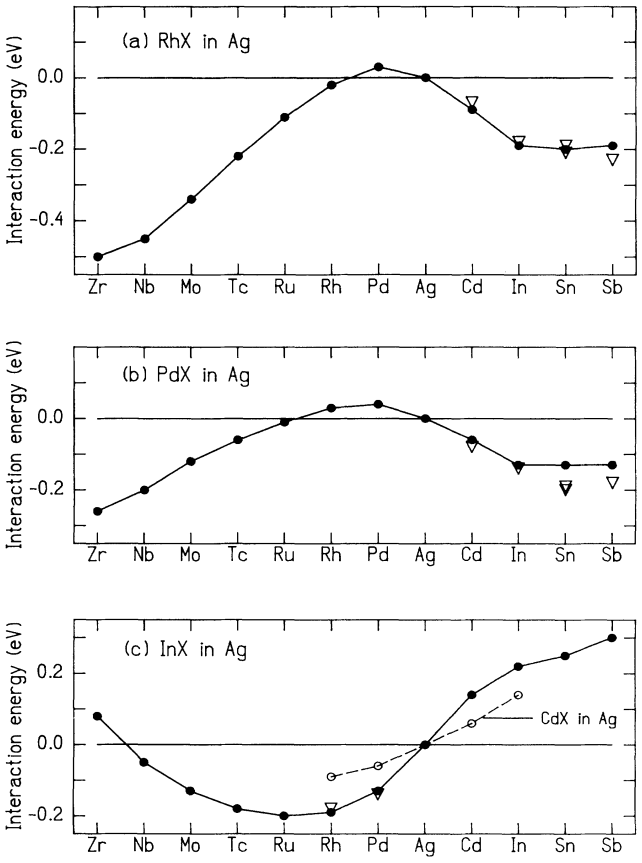

FIG. 2. Interaction energies of 4d and 5sp impurities with (a) ^{99}Rh, (b) ^{100}Pd, and (c) ^{111}In in Ag. The theoretical results (●) as well as the measured results (▽) are shown. The theoretical results (○) for Cd-X systems (X = Rh–In) are also shown in (c).

TABLE I. Interaction energies of 4d and 5sp impurities with the PAC probes ^{99}Rh, ^{100}Pd, and ^{111}In in Ag. The calculated results are shown as well as the experimental results (in eV). The negative values mean attractive interaction, positive ones mean repulsive interaction.

Impurity	Zr	Nb	Mo	Tc	Ru	Rh	Pd	Ag	Cd	In	Sn	Sb
						PAC probe ^{99}Rh						
Theory	−0.50	−0.45	−0.34	−0.22	−0.11	−0.02	0.03		−0.09	−0.19	−0.20	−0.19
Expt.									−0.07[a]	−0.18[a]	−0.21[a]	−0.23[a]
											−0.19[b]	
						PAC probe ^{100}Pd						
Theory	−0.26	−0.20	−0.12	−0.06	−0.01	0.03	0.04		−0.06	−0.13	−0.13	−0.13
Expt.									−0.08[c]	−0.14[c]	−0.19[c]	−0.18[c]
											−0.20[b]	
						PAC probe ^{111}In						
Theory	0.08	−0.05	−0.13	−0.18	−0.20	−0.19	−0.13		0.14	0.22	0.25	0.30
Expt.						−0.18[a]	−0.14[c,d,e]					

[a]Reference 16.
[b]Reference 17.
[c]Reference 18.
[d]Reference 19.
[e]Reference 20.

impurity pairs can be classified into the following three groups.

(1) For the 4*d*-4*d* pairs (^{99}Rh-*X* and ^{100}Pd-*X*, *X* = Zr–Ru), the interaction is attractive and its magnitude decreases almost linearly from Zr to Ru. The magnitudes of the interaction energies of ^{99}Rh-*X* pairs are ~2 larger than those of Pd-*X* pairs.

(2) For the 5*sp*-4*d* pairs (^{111}In-*X*, *X* = Zr–Pd), the interaction is attractive and its magnitude shows a parabolic behavior with the minimum around Ru. Analogously for the 4*d*-5*sp* pairs (^{99}Rh-*X* and ^{100}Pd-*X*, *X* = Cd–Sb), the interaction is also attractive. The magnitude increases linearly from Ag to In and is almost constant from In to Sb. It is noted that the magnitudes of the interaction for ^{99}Rh-*X* is ~1.5 larger than those for ^{100}Pd-*X* (*X* = Cd–Sb), regardless of *X*.

(3) For the 5*sp*-5*sp* pairs of ^{111}In-*X* (*X* = Cd–Sb), the interaction is repulsive and increases linearly from Ag to Sb, but with a decreased slope from In to Sb.

For all three probe atoms we obtain very good agreement with the experimental results, despite the fact that our calculations completely ignore the lattice relaxations. We believe therefore that, for the systems studied here, relaxation effects are of minor importance. First, we discuss the interaction of 4*d*-4*d* pairs in Ag, i.e., ^{99}Rh-*X* and ^{100}Pd-*X* with *X* = Zr–Pd. The basic feature shown in Fig. 2 is the strong binding of the Rh and Pd probes with *X* impurities at the beginning of the 4*d* series. The binding arises from the covalent hybridization between the 4*d* states of the probe and the ones of the impurity, leading to the formation of the bonding and antibonding virtual bound states. The attraction is strongest, if only the bonding states are occupied. This is the case for the Rh-Zr and the Pd-Y pairs, since each pair has, in total, ten *d* electrons which just occupy the ten available *d*-bonding states. For the higher valent impurities like Nb, Mo, etc., the antibonding states are also successively filled, so that the attraction strongly decreases. The stronger attraction of the Rh-*X* pairs compared to the Pd-*X* pairs has two reasons: Partly it is due to the reduced occupation of the antibonding levels for the Rh case. To a larger part it is due to the stronger hybridization, since the Rh *d* states are most extended than the Pd ones. The repulsive interaction at the end of the 4*d* series, i.e., for the Rh-Pd and Pd-Pd pairs, cannot be understood in this simple model. Here one has to compare the effectiveness of the *d*-*d* bonding of the pair with 4*d*-5*sp* bonding with the Ag host atoms which determine the reference energy for the isolated impurities. Also, the impurity *s* and *p* orbitals might play a non-negligible role in the bonding.

Next we examine the interaction of the 5*sp*-4*d* pairs, e.g., of the ^{111}In-*X* systems. The attraction between the 4*d* impurity and In can be understood by considering the gain of the band energy due to the increased broadening of the impurity virtual bound state, being induced by the In probe on the neighboring site. The parabolic behavior of the binding across the 4*d* series can be understood quite analogous to Friedel's explanation of the cohesive energies of the transition metals.[21] In the first half of the period only the bonding states are occupied, so that the binding has a maximum in the middle of the series and then decreases with the occupation of the antibonding states. Since the broadening of the virtual bound state increases with the strength of the hybridization and thus with the valence of the *sp* impurity, we expect for the Cd-*X* system about half the interaction energy as for the In-*X* system which is in agreement with the values shown in Fig. 2(c) for Cd-*X*.

The other 4*d*-5*sp* systems shown in Figs. 2(a) and 2(b), i.e., Rh-*X* and Pd-*X* with *X* = Cd–Sb, also have an attractive interaction. The binding energy first increases linearly with the valence of the *sp* impurity, as explained above, and then saturates from In to Sb. The binding of the Rh-*X* pair is about a factor 1.5 larger than the binding of Pd-*X*. This is due to the combined action of two effects, the larger extent of the Rh *d* wave function, resulting in a stronger hybridization and the reduced occupation of the antibonding states.

Now we discuss the behavior of the 5*sp*-5*sp* pairs, showing a repulsive interaction. It can qualitatively be understood by considering the electrostatic interaction of the two impurities, being properly screened by the Ag host. This can be shown either by replacing the two impurity potentials by pseudopotentials and using second-order perturbation theory or by using the expression for the interaction energy derived in Ref. 8, being based on the Hellmann-Feyman theorem with the nuclear charge as variable. By treating the changes of ΔZ_1 and ΔZ_2 of both impurities as a perturbation, the interaction energy ΔE is, in this case, given by

$$\Delta E \simeq \Delta Z_1 \, \Delta V_2(\mathbf{R}_1) \propto \Delta Z_1 \, \Delta Z_2 \ ,$$

where $\Delta V_2(\mathbf{R}_1)$ is the change of the Coulomb potential at the position $\mathbf{R}_1$, being induced by an isolated impurity with the charge excess ΔZ_2 at the neighboring site. The interaction is repulsive, since the potential $\Delta V_2(\mathbf{R}_1)$ for Cd–Sb on the neighboring site has the same sign as ΔZ_2, i.e., it is repulsive for $\Delta Z_2 > 0$. This incomplete screening of the potential on the neighboring site is the reason why two *sp* impurities are repelling each other. It also explains directly why the interaction of Cd-*X* system is about half the value of the In-*X* pair. Of course, the above expression for the interaction is based on perturbation theory and holds only for small ΔZ_i's. Therefore, the repulsive interaction for the In-*X* pair does not vary linearly with ΔZ for higher valent impurities. The above expression $\Delta E = \Delta Z_1 \, \Delta V_2(\mathbf{R}_1)$ for the interaction energy can also be applied to the 4*d*-5*sp* pairs. The derivation given in Ref. 8 requires only the excess valence ΔZ_1 (of the *sp* impurity) to be small, whereas the second defect can be a strong perturbation. In this way the interaction is determined by the change ΔV_2 of the potential of the 4*d* impurity on the neighboring host site, calculated non-perturbatively for the isolated impurity. A more detailed discussion of the trends of the interaction energies will be given elsewhere.[22] Note that, in the above discussion, the *d* band of Ag does not enter at all. We believe that it plays a minor role in the interaction, so that for this purpose the Ag host might be well described by a jellium model.

IV. CALCULATED RESULTS OF THE PROBE-IMPURITY INTERACTION ENERGIES IN Pd

In this section we discuss the calculated results for the nearest-neighbor interaction energies of the PAC probes (^{99}Rh, ^{111}In) with 4*d* and 5*sp* impurities in Pd. Figure 3 and Table II show the calculated interaction energies as well as available experimental values.[23,24] Positive energies mean repulsive interaction between the probe and impurity, negative mean attractive interaction. We note that our calculated results agree with the experimental value for the probe ^{111}In (Pd^{111}InAg), but completely disagree with those for the probe ^{99}Rh. It is noted that the calculated results are very different from those of the same pairs in Ag. This means that the role of the 4*d* states of the host Pd are very important for the probe-impurity interaction in Pd. The calculated results are summarized as follows.

(1) For the ^{99}Rh-*X* (*X* = Zr–Sb) pairs the interaction is very weak for all impurities considered. The attraction in the 4*d* impurity region shows a smooth parabolic behavior, while the repulsive in the 5*sp* impurity region is almost constant.

(2) For the ^{111}In-*X* (*X* = Zr–Sb) pairs the interaction is strongly repulsive in the whole impurity region except for impurities near Pd in the Periodic Table.

First, we discuss the interaction of the 4*d*-4*d* pairs in Pd by using a simple bond model. The change of the *d*-bond energy due to the Rh-*X* pair formation is given by

$$\Delta E = U_{\mathrm{Rh}X} + U_{\mathrm{PdPd}} - U_{\mathrm{Pd}X} - U_{\mathrm{PdRh}} ,$$

where U_{XY} is the energy of an nearest-neighbor *X*-*Y* bond. Positive values of the bond energies mean repulsive interaction, negative ones mean attractive interaction. Note that, during the pair formation, two bonds relevant for the isolated impurities ($U_{\mathrm{Pd}X}$ and U_{PdRh}) are replaced by two Rh-*X* and Pd-Pd bonds. Since for similar reasons as in the discussion for the Ag host (see Sec. III) the Rh-*X* bond is expected to be stronger than the Pd-*X* bond, the interaction should be basically attractive for the whole 4*d* series. However, the parabolic behavior seen in Fig. 3(a) cannot be explained by the bond energies alone, since these should lead to maximal bonding at the beginning of the series. Here one might invoke an additional repulsion between the ionic cores, e.g., as introduced by Pettifor[12] to discuss the cohesion of the transition metals. For the above systems this leads to an additional repulsive contribution, which is especially important at the beginning of the series, as a more detailed discussion shows.[22]

Unlike the other systems examined here, the ^{111}In probe in Pd shows a repulsive interaction with both the 5*sp* and the 4*d* impurities. For the 5*sp* impurities, the basic feature is the strength of the Pd-*X* bond which can-

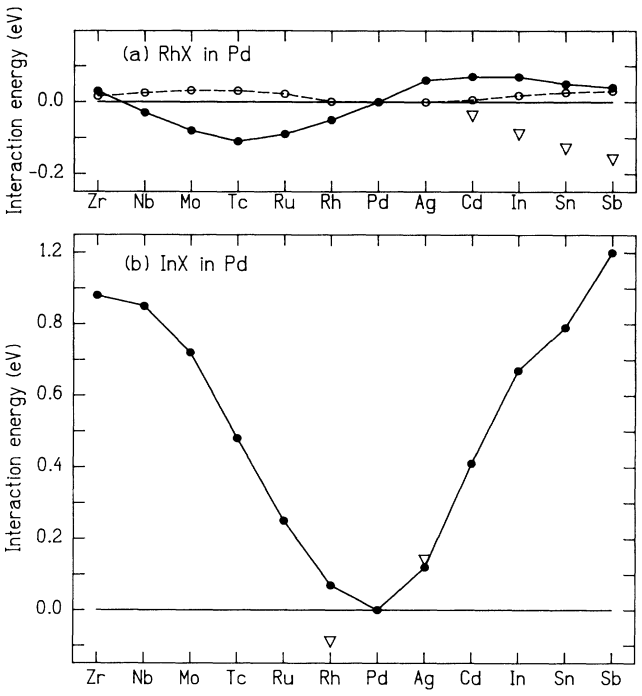

FIG. 3. Interaction energies of 4*d* and 5*sp* impurities with (a) ^{99}Rh and (b) ^{111}In in Pd. The theoretical results (●) and measured results (▽) are shown. The theoretical results (○) for second-neighbor interaction energies of Rh-*X* in Pd are also shown in (a).

TABLE II. Interaction energies of 4*d* and 5*sp* impurities with the PAC probes ^{99}Rh and ^{111}In in Pd. The calculated results are shown as well as the experimental results (in eV). The negative values mean attraction interaction, positive ones mean repulsive interaction.

Impurity	Zr	Nb	Mo	Tc	Ru	Rh	Pd	Ag	Cd	In	Sn	Sb
PAC probe ^{99}Rh												
Theory	0.03	−0.03	−0.08	−0.11	−0.09	−0.05		0.06	0.07	0.07	0.05	0.04
Expt.									−0.04[a]	−0.09[a]	−0.13[a]	−0.16[a]
PAC probe ^{111}In												
Theory	0.88	0.85	0.72	0.48	0.25	0.07		0.12	0.41	0.67	0.79	1.00
Expt.						−0.09[a]		0.14[b]				

[a]Reference 23.
[b]Reference 24.

not be overcome by the competing In-X bonds. For the In impurity in Pd, the bonding is strong because, due to the formation of bonding an antibonding states, the genuine Pd d states representing the bonding hybrides can locally be completely filled up: This may be understood by the fact that the solution energy of In in Pd is very large as shown later in Fig. 4. This effectively means that all bonding states are occupied, which is a very favorable situation for bonding. On the other hand, for the 4d impurities (X =Zr–Rh), the Pd-X bond dominates and strengthens at the beginning of the series since, due to the average valence of 5, only the 4d-4d bonding hybrides are occupied. Contrary to this, the In-X bonding is maximal for Pd and becomes progressively weaker for the other 4d elements.

By comparing with experiment we find that there is good agreement with the experimental value for the system *Pd*^{111}InAg. On the contrary, our calculations are in strong disagreement with the experiments[23] for the interaction of Rh with 5sp impurities which show a considerable binding, while the calculations predict a weak repulsion. The reason for the disagreement is not clear to us. The experimental data seem to be rather solid, e.g., the same binding energy for the *Pd*RhIn systems has been obtained by using ^{99}Rh and ^{111}In probes. One might think that while the interaction is repulsive for the nearest-neighbor site, the experimentally found binding of the pairs might be due to an attractive next-nearest-neighbor interaction. We have therefore also performed similar calculations as described in Sec. II for the second-neighbor interaction. The results are also included in Fig. 3(a) (dashed line). In general, the interaction is considerably weaker than for the first neighbor. Moreover, for the 5sp impurities the interaction with Rh is also repulsive for the second neighbor. Thus, the possibility of a more distant pair formation can be excluded. While the calculated repulsion of Rh with 5sp impurities in Pd is in disagreement with the PAC experiment, there is good evidence that the calculated attraction between two Rh impurities in Pd is correct. The Rh-Pd alloys are known to be segregation systems,[25,26] meaning that, in the dilute limit, the dominating Rh-Rh interaction has to be attractive.

Next we have to discuss the possibility that lattice relaxations due to size differences cause a sufficient large attractive contribution to the interaction to explain the difference between experiment and our calculations which do not include relaxation effects. At present we cannot exclude this possibility, however, we have doubts that this is the correct explanation. Note that, for all three probes in Ag, we obtain very good agreement with the PAC experiments, leaving little room for lattice relaxation effects of the order of -0.2 eV which are required, e.g., for the interaction of Rh with Sn or Sb in Pd. Inglot *et al.*[23] analyze the interaction by the Miedema-Królas model[4,27] which we will discuss in the next section. In the model the interaction energy is approximated by a difference of solution energies which are estimated by using Miedema's empirical formula.[5,6] Since this model also leads to a repulsive interaction between ^{99}Rh and the 5sp impurities in Pd (see Sec. V), Inglot *et al.* argue that Miedema's result for the solution energies in Pd are not sufficiently accurate, since the elastic energy due to the relaxation effects is not included. In order to examine this problem, we have calculated the solution energies of 4d and 5sp impurities in Pd and compared them with available experimental data[28,29] and with the result of Miedema.[5,6] As Fig. 4 shows, calculations, experiments, and Miedema's empirical approach all agree quite well and there is no indication of a large contribution from lattice relaxations, which are not included in our calculation and which would lower the calculated values.

In conclusion, the disagreement between calculations and experiments for the *Pd*^{99}RhX systems is puzzling, especially in view of the good agreement obtained for the other systems. An *ab initio* calculation of the lattice relaxation effects is highly desirable.

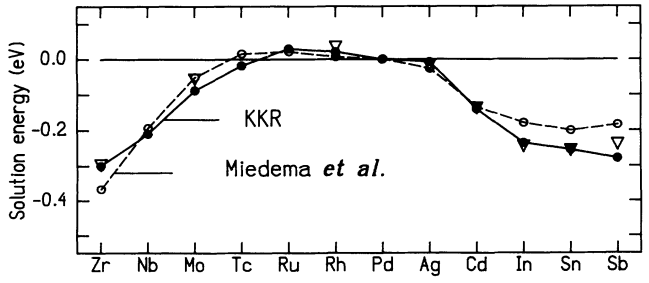

FIG. 4. Solution energies per bond of 4d and 5sp impurities in Pd. The theoretical results (●), the results of the Miedema-Królas model (○), and the measured results (▽) are shown.

V. MIEDEMA-KRÓLAS MODEL FOR THE INTERACTION ENERGY

In order to estimate the interaction energy between the probe and impurity in the metal, Królas developed a phenomenological model.[4,27] According to his way,[4] the nearest-neighbor interaction energy $E_{\rm int}$ between two impurities B and C in the host A can be rewritten in the following form:

$$E_{\rm int}=\Delta\tilde{E}_{BC}-E_s^{B\text{ in }A}-E_s^{C\text{ in }A}\ , \tag{5.1}$$

$$\Delta\tilde{E}_{BC}=\Delta E_{BC}-E_C-E_B+2E_A\ , \tag{5.2a}$$

$$E_s^{B\text{ in }A}=\Delta E_{AB}-E_B+E_A\ , \tag{5.2b}$$

$$E_s^{C\text{ in }A}=\Delta E_{AC}-E_C+E_A\ , \tag{5.2c}$$

where E_X is the energy per bond of the pure X metal and $E_s^{B\text{ in }A}$ ($E_s^{C\text{ in }A}$) is the solution energy per bond of a B (C) atom in the host A. On the other hand, it should be noted that $\Delta\tilde{E}_{BC}$, where B and C are both impurities, is not the solution energy per bond of a C atom in the host B. However, if the host A is approximated by the host B, $\Delta\tilde{E}_{BC}$ becomes the solution energy per bond, $E_s^{C\text{ in }B}$ of a C atom in the host B. This approximation seems to be allowed if the A and B atoms show a similar chemical behavior. Thus, for the systems where the probe or impurity is similar to the host atom, $E_{\rm int}$ is expressed by use of only three solution energies as follows:

$$E_{\text{int}} \sim E_s^{C \text{ in } B} - E_s^{B \text{ in } A} - E_s^{C \text{ in } A} , \quad (5.3)$$

where $E_s^{X \text{ in } Y}$ is the solution energy per bond of the impurity X in the host Y, being easily obtained by use of the semiempirical formula of Miedema *et al.*[5,6] The purpose of this section is to examine the accuracy of the approximate equation (5.3) for the interaction energies.

We first discuss the interaction energies of ^{100}Pd-X (X = Zr–Sb) pairs in Ag. The use of Eq. (5.3) seems to be allowed for this system because Pd is located next to Ag in the Periodic Table. The interaction energy is written as follows:

$$E_{\text{int}} \sim E_s^{X \text{ in Pd}} - E_s^{\text{Pd in Ag}} - E_s^{X \text{ in Ag}} . \quad (5.4)$$

The solution energies of the impurities (Zr–Sb) in Pd and Ag are shown in Fig. 5. The resulting E_{int} are shown in Fig. 6(a). We note that the approximate equation (5.4) reproduces the results obtained by the exact equation (2.2) very well. From the analysis of the three kinds of solution energies in Eq. (5.4), it is obvious that the major part of E_{int} is $E_s^{X \text{ in Pd}}$. This means that the bonds of the impurities with the transition-metal probe Pd are much stronger than those of the impurities with the nobel-metal host Ag. This is not the case for the interaction energies in the transition-metal host where the bonds between the impurities and the host atoms are also strong, as discussed in Sec. IV.

Next we discuss the interaction energies of ^{99}Rh-X (X = Zr–Sb) in Pd. The interaction energy is written as follows:

$$E_{\text{int}} \sim E_s^{X \text{ in Rh}} - E_s^{\text{Rh } in \text{ Pd}} - E_s^{X \text{ in Pd}} . \quad (5.5)$$

The solution energies of the impurities (Zr–Sb) in Rh and Pd are also shown in Fig. 5. Note that the solution energy, $E_s^{\text{Rh in Pd}}$, of Rh in Pd is very small. The resulting E_{int} are shown in Fig. 6(b). The impurity dependence of the exact results (2.2) is very well reproduced by Eq. (5.5). The smallness of E_{int} is easily understood by a systematic cancellation of $E_s^{X \text{ in Rh}}$ and $E_s^{X \text{ in Pd}}$, due to the similarity of the individual characters of Rh and Pd elements.

Lastly we discuss the strong repulsion of ^{111}In-X (X = Zr–Sb) pairs in Pd. For this system, the replacement of $\Delta E_{\text{In}X}$ by $E_s^{X \text{ in In}}$ is not allowed because the individual character of ^{111}In is very different from that of the host atom Pd. However, if the impurity X is located next to Pd in the Periodic Table, the replacement of $\Delta E_{\text{In}X}$ by $E_s^{X \text{ in In}}$ may be allowed. Thus, the interaction energy E_{int} may be written as follows:

$$E_{\text{int}} \sim E_s^{\text{In in } X} - E_s^{\text{In in Pd}} - E_s^{X \text{ in Pd}} . \quad (5.6)$$

It is obvious in Fig. 6(c) that only for the impurities X = Rh or Ag can the results of Eq. (2.2) be very well reproduced by the approximate equation (5.6). However, it should also be noted that Eq. (5.6) can reproduce at least qualitatively the chemical trends of the repulsive interaction energies in the whole impurity region. The analysis of solution energies shown in Fig. 5 may substantiate the explanation discussed in Sec. IV: The strong repulsion, except for X = Rh and Ag, originates in the energy loss due to the break up of the two bonds Pd-X and Pd-In.

In conclusion, the Miedema-Królas model works for the systems where the individual character of the impurity or probe atom is similar to that of the host and may be helpful for the qualitative discussions of those interaction energies.

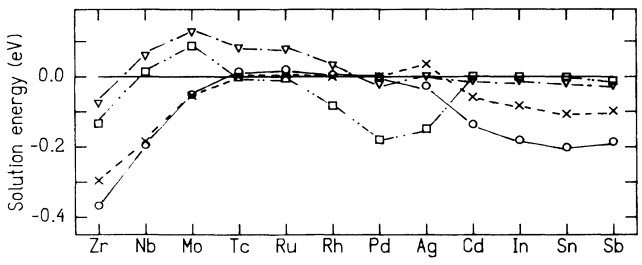

FIG. 5. Solution energies per bond of 4*d* and 5*sp* impurities in Pd (○), Rh (×), Ag (▽), predicted by the semiempirical formula of Miedema *et al.* The solution energies (□) of an In impurity in the hosts X (X = Zr–Sb) are also shown.

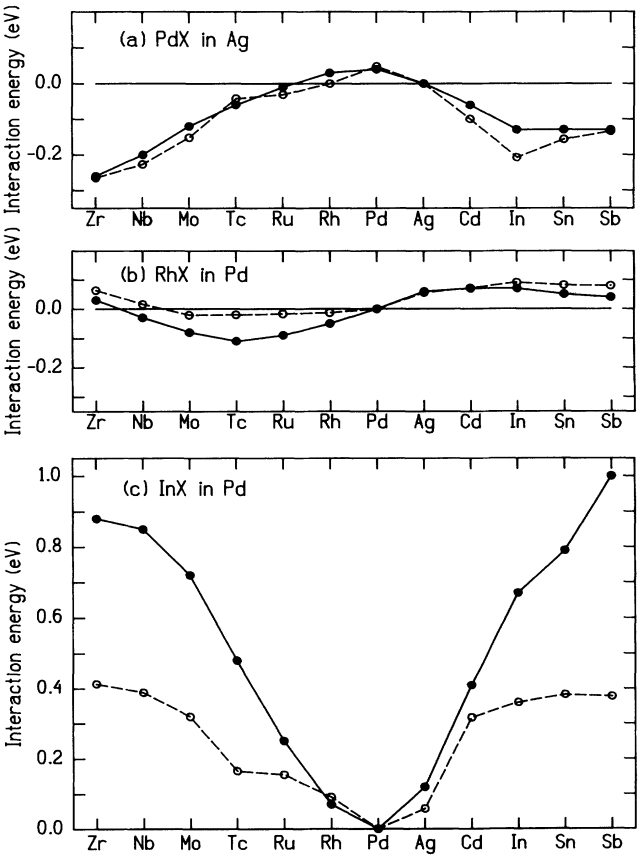

FIG. 6. Interaction energies (○) of 4*d* and 5*sp* impurities with (a) ^{100}Pd in Ag, (b) ^{99}Rh in Pd, (c) ^{111}In in Pd, predicted by the Miedema-Królas model. The results of the KKR calculations (●) are also shown for comparison.

VI. SUMMARY AND CONCLUSION

The aim of the paper was to present accurate data for the interactions between the PAC probes (^{99}Rh, ^{100}Pd, ^{111}In) and impurities (Zr–Sb) in Ag and Pd and to elucidate the physical mechanisms responsible for the interaction. In order to minimize the effect of lattice relaxations, not included in the present calculations, we considered only the hosts and impurities from the same row of the Periodic Table as the PAC probes. We apply density-functional theory in the local-density approximation and solve the Kohn-Sham equations by using the KKR Green's-function method for impurity calculations.[8–10]

In Ag, the Rh and Pd probe atoms show a very similar behavior, an attraction to the 5*sp* atoms and an even stronger attraction to the elements at the beginning of the 4*d* series, like Y, Zr, and Nb. In contrast to this, the In probe interacts repulsive with the 5*sp* impurities, but is attracted by the elements in the middle of the 4*d* series. The calculated energies are in good agreement with the binding energies determined by PAC experiments. A detailed discussion of the physical origin of the binding and repulsion is given.

In Pd, the In probe is strongly repelled both from 5*sp* impurities as well as from 4*d* impurities. For the Rh probe we obtain a weak attraction to the 4*d* impurities varying parabolically across the series and a weak repulsion from the 5*sp* impurities. The latter results are in disagreement with experiment. The reason for the disagreement is not understood. In order to make progress in this field, a reliable calculation of the lattice relaxation and the resulting elastic interaction energy is necessary.

ACKNOWLEDGMENT

One of the authors (T.H) would like to thank T. Asada for helpful discussions.

[1]K. Królas, Hyperfine Interact. **59**, 58 (1990).
[2]A. Blandin, J. L. Deplante, and J. Friedel, J. Phys. Soc. Jpn. **18**, Suppl. II, 85 (1963).
[3]J. L. Deplante and A. Blandin, J. Phys. Chem. Solids **26**, 381 (1965).
[4]K. Królas, Phys. Lett. **85A**, 107 (1981).
[5]A. R. Miedema, P. F. deChatel, and F. R. de Boer, Physica B **100**, 1 (1980).
[6]F. R. de Boer, R. Boom, W. C. M. Mattens, A. Miedema, and A. K. Niessen, in *Cohesion in Metals,* edited by F. R. de Boer and D. G. Pettifor (North-Holland, Amsterdam, 1985), Vol. 1.
[7]U. Klemradt, B. Drittler, R. Zeller, and P. H. Dederichs, Phys. Rev. Lett. **64**, 2803 (1990).
[8]U. Klemradt, B. Drittler, T. Hoshino, R. Zeller, P. H. Dederichs, and N. Stefanou, Phys. Rev. B **43**, 9487 (1991).
[9]P. J. Braspenning, R. Zeller, A. Lodder, and P. H. Dederichs, Phys. Rev. B **29**, 703 (1984).
[10]B. Drittler, M. Weinert, R. Zeller, and P. H. Dederichs, Phys. Rev. B **39**, 930 (1989).
[11]J. A. Majewski and P. Vogl, in *Cohesion and Structure,* edited by F. R. de Boer and D. G. Pettifor (North-Holland, Amsterdam, 1989), Vol. 2, p. 287.
[12]D. G. Pettifor, in *Solid State Physics,* edited by H. Ehrenreich and D. Turnbull (Academic, New York, 1987), Vol. 40, p. 43.
[13]R. Zeller, J. Deutz, and P. H. Dederichs, Solid State Commun. **44**, 993 (1982).
[14]U. Klemradt, Diploma thesis, *Kernforschungsanlage Jülich* (unpublished).
[15]V. R. Moruzzi, J. F. Janak, and A. R. Williams, *Calculated Electronic Properties of Metals* (Pergamon, New York, 1978).
[16]K. Królas, W. Bolse, and L. Ziegeler, Hyperfine Interact. **35**, 635 (1987).
[17]R. Kmiec, A. Z. Hrynkiewicz, K. Królas, and K. Tomala, J. Phys. F. **17**, 1349 (1987).
[18]K. Królas, P. Heubes, G. Schatz, and A. Weidinger, Hyperfine Interact. **35**, 619 (1987).
[19]K. Królas, B. Wodniecka, and P. Wodniecki, Hyperfine Interact. **4**, 605 (1978).
[20]I. J. R. Baumvol, M. Behar, J. A. H. da Jornada, R. P. Livi, K. W. Lodge, A. Lopez-Gracia, and F. C. Zawislak, Phys. Rev. B **22**, 5115 (1980).
[21]J. Friedel, in *The Physics of Metal I,* edited by J. M. Ziman (Cambridge University Press, London, 1969).
[22]T. Hoshino *et al.* (unpublished).
[23]Z. Inglot, D. Wegner, K. Królas, and L. Ziegler, J. Phys: Condens. Matter **2**, 1435 (1990).
[24]Z. Inglot, A. Z. Hrynkiewicz, K. Królas, and P. Wodniecki, Hyperfine Interact. **35**, 639 (1987).
[25]See, e.g., the binary phase diagram of Pd-Rh in F. R. de Boer, R. Boom, W. C. M. Mattens, A. Miedema, and A. K. Niessen, *Cohesion in Metals* (Ref. 6), p. 478.
[26]M. Hansen and K. Anderko, *Constitution of Binary Alloys* (McGraw-Hill, New York, 1958).
[27]T. E. Cranshaw, J. Phys. F. **17**, 1645 (1987).
[28]R. Hultgren, P. D. Desai, D. T. Hawkins, M. Gleiser, and K. Kelly, *Selected Values of Thermodynamic Properties of Metals and Alloys* (Americal Society of Metals, Metal Park, OH, 1973).
[29]O. Kubaschewsky and C. B. Alcock, *Metallurgical Thermochemistry* (Pergamon, Oxford, 1979).